Proceedings of IMECE2006
2006 ASME International Mechanical Engineering Congress and Exposition
November 5-10, 2006, Chicago, Illinois, USA

IMECE2006-14051

EXPERIMENTAL DESIGN AND ANALYSIS OF BIMORPHS AS SYNTHETIC JET DIAPHRAGMS

Poorna P. Mane
Virginia Commonwealth University
601 West Main Street
Richmond, Virginia 23284-3015
manepp@vcu.edu

Karla M. Mossi
Virginia Commonwealth University
601 West Main Street
Richmond, Virginia 23284-3015
kmmossi@vcu.edu

Robert G. Bryant
NASA Langley Research Center
MS 226,
Hampton, VA 23681
r.g.bryant@larc.nasa.gov

ABSTRACT

Synthetic jet actuators are promising Active Flow Control (AFC) devices which could lead to saving millions of dollars in fuel consumption each year. The Bimorph piezoelectric actuators are an attractive alternative to other type of actuators as active diaphragms and are the focus of this work. Among the properties of a Bimorph actuator, a number of geometrical and physical external factors may have an effect on its performance as a synthetic jet actuator. Using statistical tools some of the physical and geometrical factors are evaluated as independent variables that may have an effect on the synthetic jet peak velocity, the dependent variable. Among the factors studied are the geometry of the synthetic jet cavity, the driving signal used to operate the active diaphragm, and the effect of a pressure gradient on the device. Among the six factors considered, the driving signal was found to have the highest effect on the peak jet velocity, and the factor of frequency proved to have a smaller effect. The cavity geometrical parameters were also relevant, a smaller orifice and a smaller cavity produce higher peak jet velocities. An adverse pressure gradient was also found to have a significant effect on peak jet velocity, diminishing its magnitude with increasing pressure.

NOMENCLATURE

C_H	cavity height
D_o	orifice diameter
E	voltage
F_Z	driving signal
P_B	passive cavity pressure
X_i	factors
Y_i	responses
f	frequency
i	factor no.
j	run no.
n	number of runs
r_o	orifice radius
x_i	individual factor
y_j	response per run (j)
y_j^+	high level responses
y_j^-	low level responses
Δx_i	effect estimate per factor (i)

INTRODUCTION

Methods that attempt to control the motion of fluids have been extensively explored in the past. These methods can be passive or active or both (Gad-el-Hak 2000). Passive flow control is usually achieved through careful modifications to the existing system using steady state tools such as wing flaps, spoilers and vortex generators, among others. These techniques, though effective, have marginal power efficiency and are not capable of adjusting to the instantaneous flow

conditions experienced during flight. Active flow control (AFC) methods however, are much more efficient. Through AFC, the flow field around a body can be modified to match the constantly changing conditions of an unsteady flow field by introducing small amounts of energy locally to achieve non-local changes in the flow field with large performance gains (Amitay et al. 1998, Kral et al. 1997, Smith & Glezer 1998).

The feasibility of increasing the efficiency and simplifying fluid related systems is very appealing considering that a one percent saving in world consumption of jet fuel is worth about 1.25 million dollars a day of direct operating costs (Collis et al. 2004). Likewise, such fuel savings would lead to reduced environmental impact, although such environmental effects are difficult to quantify. Mclean et al. evaluated different AFC concepts and applications were considered for civil jet transports (McLean et al. 1999). The simplification of conventional high lift systems by AFC was identified as a prime candidate, possibly providing 0.3% airplane cost reduction, up to 2% weight reduction and about 3% cruise drag reduction. Also the advent of MEMS (Micro Electro Mechanical Systems) technology in the last two decades has provided a new impetus to the field of active control (Ho & Tai 1996).

In spite of all the advantages, using active flow control devices usually adds complexity in design, increases manufacturing and operation cost, which prevents their use. For this reason, many researchers have focused on designing better active flow control devices that are easy to manufacture, are small in size and require little power to operate. One of the devices that fulfill all of these qualities is called synthetic jets.

Synthetic jets consist of a cavity with an oscillating diaphragm. When the diaphragm oscillates air is pushed out an orifice forming a jet (Smith 1999). The jets are so called because they are synthesized from a train of vortex rings or pairs, formed from the external fluid, without net mass addition. This is one attractive feature of these devices since no hardware is required to obtain mass and flow from a separate source. The jets are formed from the working fluid of the flow system from which they are deployed. The interaction of the jets with an external flow leads to the formation of closed re-circulating flow regimes near the surface. This interaction can act as a “virtual surface” and consequently is an apparent modification of the flow boundary (Amitay et al. 1997). An array of such microfabricated devices can produce a large jet velocity if the orifices are at the correct spacing and the driving signals are in phase. The oscillating diaphragm used in the synthetic jet cavity is usually driven using electrical or mechanical power. In the past, researchers have used compressed air or regulated blowers as a means of supplying steady or oscillating flow (Seifert et al. 1993, Seifert et al. 1996). This adds to the complexity and weight of the system. Piezoelectric disks that oscillate in the same manner as a piston or a shaker when driven with an AC electric signal seem like an attractive alternative if the shaker or a piston can be eliminated to reduce the number of moving parts. Because of these advantages, several investigators have adopted piezoelectric disks as oscillating diaphragms in synthetic jets to attempt to make the systems lighter, increase efficiency and save resources (Crook et al. 1999, Rathnasingham & Breuer 1997, Smith & Glezer 1998).

The most commonly used piezoelectric diaphragm consists of a Lead Zirconate Titanate (PZT) disk bonded to a metal shim using a conductive epoxy, a Unimorph®. Although these piezoelectric disks have been successful in generating high velocities capable of altering the flow fields, the devices operate best at high resonance frequencies, limiting the range of operation of the synthetic jet. Also, after a period of time, the PZT disk would start to delaminate and/or the output of the device would drop and the resonant frequency would change. Part of the degradation of performance of the device with time may be due to a combination of small cracks appearing in the bond line and the growth of a thin oxide layer between the brass and the conductive electrode (Bryant 1996).

The ideal piezoelectric synthetic jet is unobtrusive, consumes low power, is light, and depending on the flow conditions, can be adjusted by changing frequency of operation.

In the current study a piezoelectric laminate, Bimorph, is used as the active diaphragms in the jet cavity. Besides being lightweight, and having low power consumption, this laminate has the ability to produce micro scale displacements and provide a wide bandwidth response. Such advantages make the Bimorphs suitable for flow control purposes as demonstrated by Mossi et al. (Mossi & Bryant 2004a & b, Mossi et al. 2005a).

The promising potential of piezoelectric synthetic jets for flow control has motivated researchers at various universities, industrial laboratories and government institutions to continue to invest time and effort into their further development since synthetic jets have potential applications ranging from jet vectoring (Smith & Glezer 1997), mixing enhancement (Chen et al. 1999, Davis & Glezer 1999), to active control of separation and turbulence in boundary layers (Amitay et al. 1998, Crook et al. 1999).

Although numerical investigations are capable of providing insight into the operation of a synthetic jet, a parametric study of the flow configuration through experiments is necessary to validate the results. Experimentation however is a time consuming and expensive proposition. Design of experiments theory provides an alternative. Through a series of screening experiments, this study aims at identifying the important factors on the operation of a synthetic jet driven with a Bimorph device. The selected factors are then used in developing a regression model that quantifies the dependence of the desired response on the existing factors. Through screening experiments, statistics, and regression models a response surface of the relevant factors can be created to optimize the performance of the jet. These factors can then be incorporated on numerical models of the entire flow field for optimization.

EXPERIMENTAL SETUP

It has been proven that the boundary conditions that a piezoelectric actuator is subjected to, have a significant impact on the final performance of the device. For instance Liew states that different boundary conditions and applied voltages affect the shape control of piezo laminated composite beams (Liew et al. 2002). For this reason the clamping mechanism used becomes critical to the characterization of the synthetic jet actuator and special considerations are utilized during its design.

Series-type Bimorphs consist of two thin ceramic sheets bonded with their poling directions opposed and normal to the interface. When an electric field is applied through the bimorph, one of the plates expands while the other contracts. This mechanism creates a bending mode that mimics piston like displacement. Bimorphs are capable of generating large bending displacements of several hundred micrometers on center or edge, but the response time (1 ms) and the generative force (1.0 N) are low (Dogan et al. 2001). In the current study, the Bimorphs used are model T216-A4NO-573X manufactured by Piezoelectric Systems Inc. They consist of two nickel electroded PZT 5A discs with diameters of 63.5 mm and a total thickness of 0.41mm. They have a capacitance of 130nF at 1kHz and have been shown to produce displacements up to 0.3 mm at low frequencies (Mossi et al. 2005b). A schematic of the disc alignment along with the final shape is shown in Fig. 1.

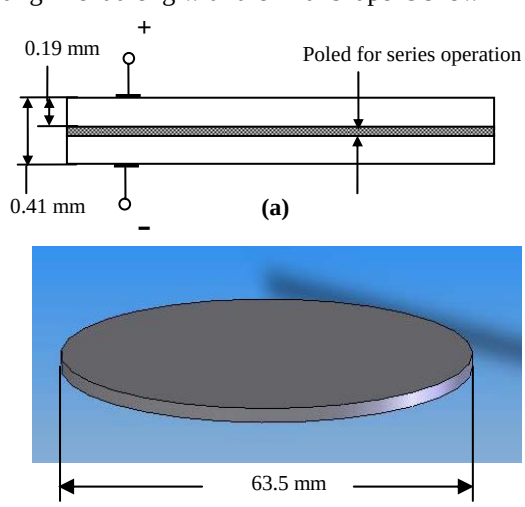

(b)

Figure 1 Bimorph (a) layer alignment, (b) final shape

The synthetic jet cavity is shown in Fig. 2. This cavity setup allows variations in cavity height and orifice. The two cavities used in the study have overall dimensions of 89.0 x 89.0 x 19.1mm and 89.0 x 89.0 x 15.1mm, which correspond to cavity heights of 9.5mm and 5.5mm respectively. This cavity height, C_H, is measured from the diaphragm to the orifice exit. The cavity housing is composed of two identical rectangular Plexiglas™ pieces with a circular aperture and a cover plate with an orifice. The two plastic pieces have 3.18mm deep circular grooves along the circumference of the aperture. The diaphragm is placed in this groove between the two pieces with neoprene rubber around the perimeter of the diaphragm on either side. Seven 3.18mm screws hold the two plastic housings and the cover plate together and clamp the actuator in place. Two cover plates with circular orifices have approximate diameters, D_0, of 2.0mm (small) and 3.67mm (large) are used. With the two cavity sizes and two orifice diameters, four different cavity configurations are possible.

The assembled actuator-cavity is mounted onto an adjustable height gauge, with the actuators surface perpendicular to the IFA100 hot-wire anemometer used to measure velocity of the jet. The diaphragm is powered with a HP function generator and a Trek amplifier model PZD-700. The entire system is controlled using a data acquisition system run by Labview®.

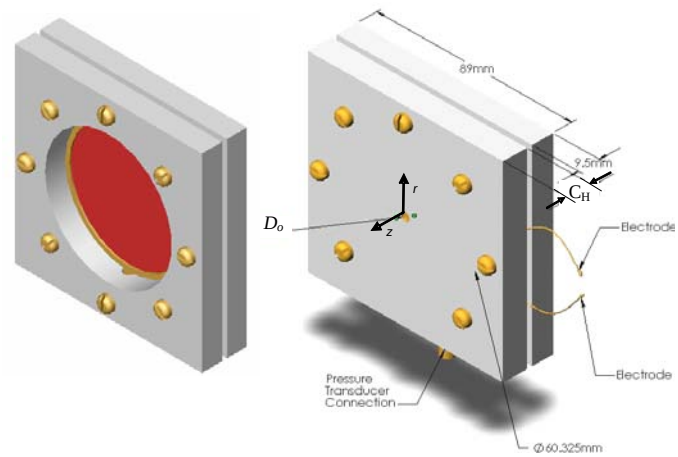

(a) (b)

Figure 2 Synthetic Jet Cavity (a) final assembly, (b) clamped actuator

In one set of experiments the passive cavity of the synthetic jet actuator is pressurized to desired levels to tests the effects on jet velocity. This is accomplished using compressed air controlled by a pressure regulator.

Using the setup described above certain factors are chosen to be studied. These include the driving signal, voltage, frequency, cavity height, orifice diameter and the passive cavity pressure. These factors are chosen based on previous research by Mossi et al. and also during a through a literature review on the subject. The same factors are used in the regression analysis wherein each factor has two levels. All the results and statistical analysis is shown in the following sections.

EXPERIMENTAL RESULTS

Previous studies on synthetic jets have used a sinusoidal waveform as the driving input signal. A sine wave as the driving input requires relatively high frequencies matching the actuators resonance frequency to enable the formation of a

synthetic jet with significant velocity magnitude. High frequencies however, consume more power and also physically limit the oscillation amplitude of the piezoelectric diaphragm that in turn limits the amount of air volume displaced. A sawtooth signal however consists of a number of different frequency sine waves capable of providing the force required to produce large velocities at low operating frequencies. In a previously published study by Mossi et al. (2005b) the sawtooth driving signal is observed to produce higher velocities compared to the sine signal at similar operating conditions. Thus the two driving signals, sine and sawtooth, were used to drive the Bimorph.

A typical velocity curve formed with a sine wave is shown in Fig. 3. Two jets are observed with the second jet smaller in magnitude. The first jet (larger jet) follows the leading edge of the input signal and the second jet (smaller jet) follows the trailing edge. The larger jet is believed to occur during the expulsion cycle, while the smaller jet is believed to occur during the ingestion cycle. Previous studies on the synthetic jet flow fields by Glezer et al. have indicated that during the ingestion cycle the flow reenters the cavity from the sides of the orifice. Thus the velocity profile of second jet could be due to the nonparallel direction of the flow, relative to the hotwire, entering the cavity. At lower frequencies, only one jet is formed indicating that at lower frequencies the flow during ingestion cycle is nearly parallel to the hotwire anemometer and hence cannot be detected with the setup utilized here.

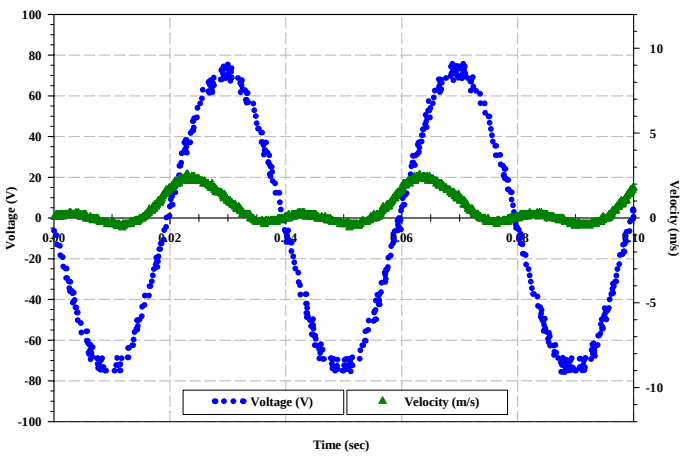

Figure 4 Typical velocity curve with a sine driving signal at 100Hz and 150Vpp

In the case of the sawtooth signal a single velocity jet is formed. As shown in Fig. 4, the jet follows the leading edge of the input signal, with series of smaller jets immediately following the first jet. These jets may be caused by vibrations of the clamped actuator. The jets formed using sawtooth driving signals are larger in magnitude as compared to the ones formed with a sine wave at comparable frequencies at the same voltage levels.

The amplitude of the driving signal also has an effect on the maximum jet velocity as seen in Fig. 5. An increase in the input voltage produces greater velocities. This effect is seen at all frequencies for both the studied driving signals. The maximum voltages the Bimorphs were driven at were below the maximum allowed voltage for each device to avoid damage to the actuator.

To test the effects of frequency on velocity, the Bimorph is operated at various frequencies up to 100Hz. As seen in Fig. 6 with a sine wave input signal the velocity increases as frequency increases. But with a sawtooth signal the trend was very different with the velocity reaching a constant value at approximately 10Hz. The reason for such behavior with the sawtooth signal may be due to a condition called "choking of the flow." This is a condition seen in nozzle flows (John 1984). If the flow is fast enough, the pressure in the restriction drops to zero, so the flow is limited to this rate regardless of the pressure in the back of the restriction.

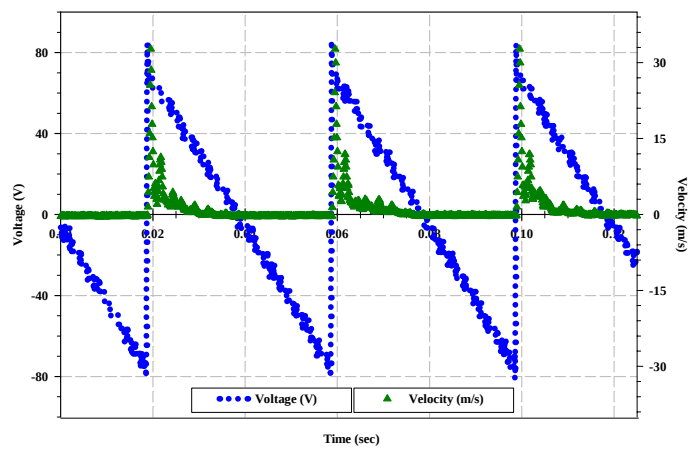

Figure 3 Typical velocity curve with a sawtooth driving signal at 25Hz and 150Vpp

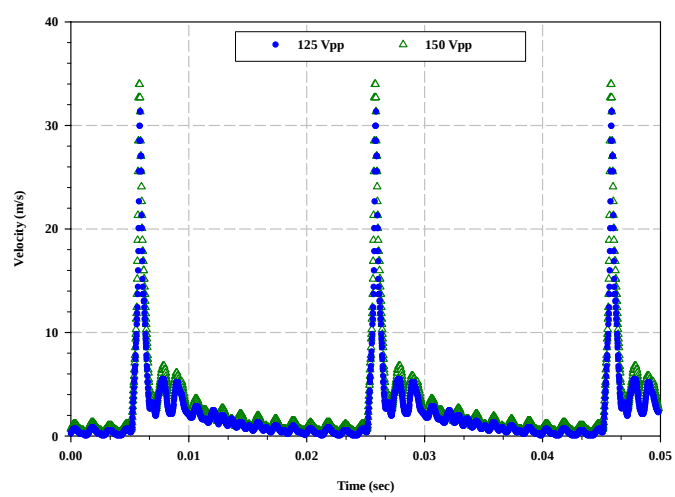

Figure 5 Effect of voltage on velocity magnitude at 50Hz using a sawtooth driving signal

The phenomenon of choking exists only in compressible flow and can occur in several flow situations. With a sawtooth signal a saturation point could be reached making the fluid in the cavity compressible and restricting the velocity through the cavity. Due to the additional force, or rapid acceleration, present in the sawtooth signal, this saturation point is reached at a low frequency. It is possible that a similar choking condition could occur with a sine signal at much higher frequencies above the ranges tested in the current study. Another explanation for such behavior with a sawtooth signal could be the resonant cavity frequency. Using the standard Helmholtz Frequency equation the resonant frequencies of the cavities were calculated in the range of 900 – 2300Hz. The driving frequency of the actuator is not close to matching the cavity frequency values; hence a more detailed study of the frequencies embedded on the sawtooth signal is needed to assess this effect though not the focus of this work.

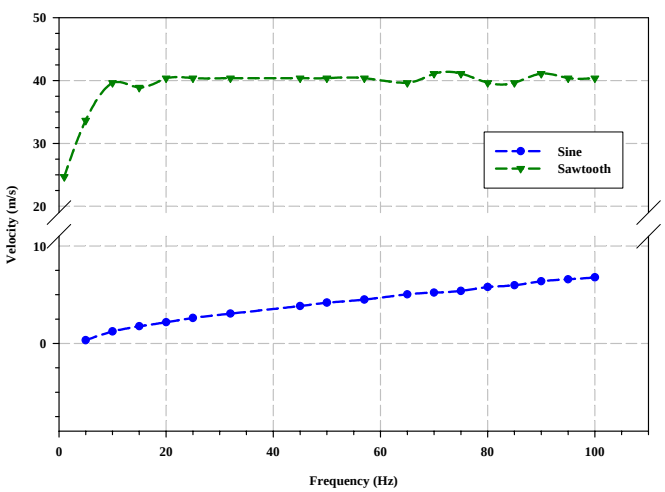

Figure 6 Frequency effects at 150Vpp

Next, the geometrical factors of the synthetic jet cavity such as cavity volume and orifice size are tested. As described before, four cavity configurations are studied as given in Tab. 1. Changing the cavity height leads to changing the volume of the cavity, thus the effects of changing the volume of the cavity are studied. The cavities with smaller volumes form higher velocities irrespective of the driving waveform used. Since cavity III and cavity IV have the same orifice diameter but different cavity heights their profile comparison will show the effects of changes in cavity height or cavity volume on the velocity magnitudes. Profiles for cavity III and cavity IV are shown in Fig. 7. Cavity III produces approximately 30% higher velocities then cavity IV with a sine signal. Similarly cavities I and II were also compared but the differences were higher at 33%. This could be due to the smaller orifice size in cavities I and II. Similar differences are observed in all cases irrespective of the driving signal, frequency or voltage. With the sawtooth signal the differences are smaller compared to the sine signal.

Similarly to test the effects of orifice diameter cavities I and III are tested as they differ in the orifice size only. It is observed that the smaller orifice diameter (smaller D_o), cavity I, produces 63% higher velocities than cavity III, larger D_o. Figure 8 shows the comparison between cavities I and III with a sine signal at 50Hz and 150Vpp. This result is expected since to maintain a constant mass flow rate, the velocity through the smaller orifice has to be higher than the larger orifice. Similar trends are observed in the comparison between cavities II and IV with differences of 61%. In case of the sawtooth driven profiles, the differences in velocities are much smaller where only 17% differences are seen in cavities I and III. Similar behavior is observed in all cavities and diaphragms tested. These results indicate that the synthetic jet velocity is dependent on the type of driving signal used.

Table 1 Cavity parameters

		C_H (mm)	
		5.50	9.55
D_o (mm)	2.00	Cavity I	Cavity II
	3.67	Cavity III	Cavity IV

The last factor investigated is passive cavity pressure. Passive cavity pressure had an adverse effect on the peak jet velocities as shown in Fig. 9. As the pressure in the back was increased the velocity decreases until it goes down to zero regardless of the driving signal, frequency or voltage used.

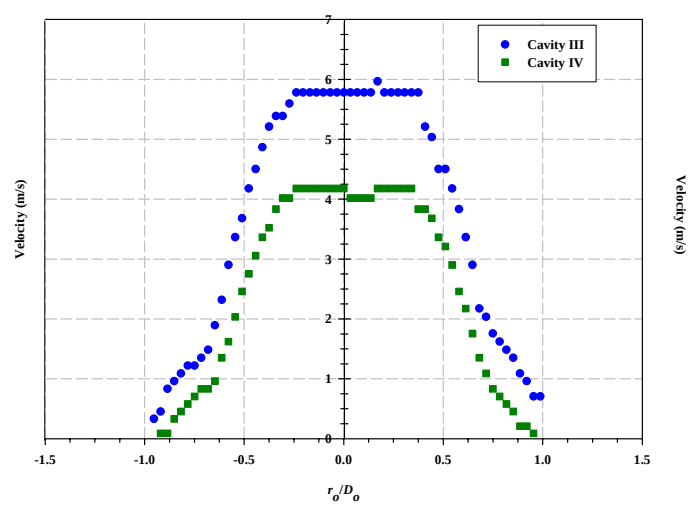

Figure 7 Cavity height effects with a sine driving signal at 50Hz and 150Vpp

STATISTICAL FACTOR ANALYSIS

In an experiment, one or more variables or factors are deliberately changed in order to observe the effect the changes have on one or more response variables. Experimental data are then used to derive an empirical model linking the outputs and inputs. These empirical models generally contain first and

second-order terms. Screening designs are used to identify the few significant factors from a list of many potential ones. In short, screening designs are economical experimental plans that focus on determining the relative significance of many main effects. This can be achieved using factorial designs (Montgomery 2005).

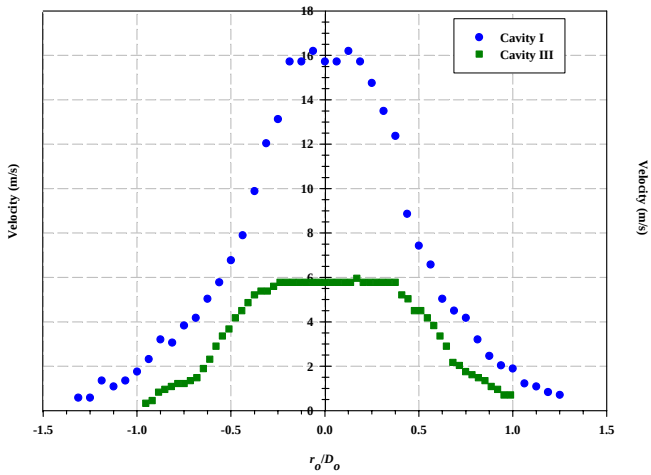

Figure 8 Orifice diameter effects with a sine driving signal at 50Hz and 150Vpp

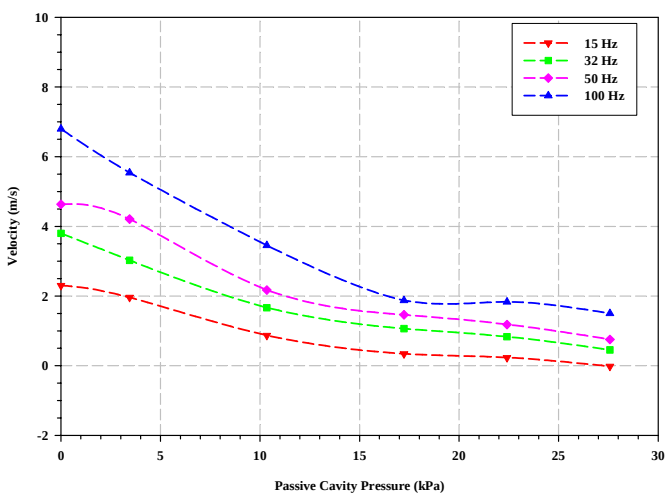

Figure 9 Passive cavity pressure effects on peak velocity at 150Vpp using a sine driving signal

The basic purpose of a factorial design is to economically investigate cause-and-effect relationships of significance in a given experimental setting. By a factorial design, each complete trial or replication of the experiment for all possible combinations of the levels of the factors are investigated. The effect of a factor is defined to be the change in response produced by a change in the level of the factor. This is called a main effect as it refers to the primary factors or interest in the experiment. For some experiments, it is seen that the difference in response between the levels of one factor is not the same at all levels of the other factors. When this occurs, there is an interaction between the factors. As the number of factors in a 2^k factorial design increases, the number of runs required for a complete replicate of the design rapidly outgrows the resources of most experimenters. If the experimenter can reasonably assume that certain high-order interactions are negligible, information on the main effects and low-order interactions may be obtained by running only a fraction of the complete factorial experiment. Since we are able to choose fractions of a full design, the whole experimental research process is made more economical and efficient. These fractional factorial designs are among the most widely used types of designs for product and process design and for process improvement.

Screening experiments are usually performed in the early stages of a project when many of the factors initially considered may have little or no effect on the response. The factors identified as important are then investigated more thoroughly in subsequent experiments. It is common to begin with several discrete or continuous input factors that can be controlled, that is, varied when desired by the experimenter and one or more measured output response variables which always are assumed to be continuous. In the current study, five factors were considered, driving waveform, voltage, frequency, cavity height, and orifice size. The peak velocity of the jet is used as the response variable. A two level design is chosen due to the large number of factors involved. In a two factor experimental design each factor has two levels. These levels "low" and "high" are denoted by "–" and "+" respectively. The high and low level values differ for each diaphragm. A typical table showing the factor distribution, levels and types is given in Tab. 2. A full factorial design requires 2^5 = 32 runs without center points or repetitions. Instead, a fractional factorial design, 2^{5-1}, was considered requiring a total of 16 observations. An additional factor is added to this design to get a modified fractional factorial design having 24 runs. The complete experimental design is shown in Tab. 3. All the runs and their characteristics are shown such that the influence of each factor can be assessed individually.

Table 2 Factor distribution

Factors	Symbols	Low Level (-1)	High Level (+1)	Units	Types
Driving Waveform	F_z	Sawtooth (-1)	Sine (+1)	None	Discrete
Applied Voltage	E	125 (-1)	150 (+1)	V_{pp}	Continuous
Frequency	f	25 (-1)	50 (+1)	Hz	Continuous
Orifice Size	D_o	2 (-1)	3.67 (+1)	mm	Continuous
Cavity Height	C_H	5.5 (-1)	9.5 (+1)	mm	Continuous
Passive Cavity Pressure	P_B	0 (-1)	55 (+1)	kPa	Continuous

From the entries in Table 3 all factor effects such as main effects, first-order interaction effects among factors, etc can be calculated. To compute the main effect estimate of a factor, the average response at all runs at the 'high' setting are subtracted from the average response of all runs set at 'low' for that particular factor.

Table 3 Fractional factorial experimental design

Run No.	Factors (X_i)						Response$_j$
j	F_z	E	f	D_o	C_H	P_B	Y_j
1	-1	-1	-1	-1	1	-1	y_1
2	1	-1	-1	-1	-1	-1	y_2
3	-1	1	-1	-1	-1	-1	y_3
4	1	1	-1	-1	1	-1	y_4
5	-1	-1	1	-1	-1	-1	y_5
6	1	-1	1	-1	1	-1	y_6
7	-1	1	1	-1	1	-1	y_7
8	1	1	1	-1	-1	-1	y_8
9	-1	-1	-1	1	-1	-1	y_9
10	1	-1	-1	1	1	-1	y_{10}
11	-1	1	-1	1	1	-1	y_{11}
12	1	1	-1	1	-1	-1	y_{12}
13	-1	-1	1	1	1	-1	y_{13}
14	1	-1	1	1	-1	-1	y_{14}
15	-1	1	1	1	-1	-1	y_{15}
16	1	1	1	1	1	-1	y_{16}
17	-1	-1	-1	1	1	-1	y_{17}
18	1	-1	-1	1	1	1	y_{18}
19	-1	1	-1	1	1	1	y_{19}
20	1	1	-1	1	1	-1	y_{20}
21	-1	-1	1	1	1	1	y_{21}
22	1	-1	1	1	1	-1	y_{22}
23	-1	1	1	1	1	-1	y_{23}
24	1	1	1	1	1	1	y_{24}

This estimate is shown in Eq. (1).

$$\Delta x_i = \frac{2}{n}\left[\sum_{j=1}^{n} y_j^{+} - \sum_{j=1}^{n} y_j^{-}\right] \qquad \textbf{Equation (1)}$$

Where Δx_i is the effect estimate, y_j^{+} are all the responses with a high effect level for the corresponding effect; y_j^{-} are all the responses with a low effect level for the corresponding effect and n is the total number of runs. Similarly the interactions effects can also be estimated. Statistical results are used to assess the validity and influence of the particular effect on the response.

The regression analysis of the factors is shown in Tab. 4. The first part of the table shows a summary output of the regression. The R-square value is the relative predictive power of a linear model. The model shown has an R-square value of 0.9264 and an adjusted R-square of 0.9109 indicating that 92% of the data can be predicted using the linear model. The adjusted R-square value is a better estimate of the model as it accounts for the size of the model as well. This is unlike the R-square value, which increases as the number of factors increase even though they might not have an effect on the experiment.

Following the summary of the linear regression, Table 4 shows the Analysis of Variances (ANOVA). The ANOVA aids in determining the validity of the experimental design by testing the difference between two or more groups. When the F-value is larger than the *Significance F*-value, the experiment design is considered to be valid, indicating that at least one of factors have an effect on the response variable. The F-value shown in Tab. 4 is computed from the mean square values, and *Significance F*-value is selected from the F-distribution tables based on the size of the sample, the number of factors, and the significance level selected which is 95% in this case. As the F-value is larger than the *Significance F*-value, the linear model design is considered to be valid.

Table 4 Regression analysis

SUMMARY

Regression Statistics	
Multiple R	0.96249
R Square	0.92638
Adjusted R Square	0.91088
Standard Error	5.0128
Obs.	24

ANOVA

	df	*SS*	*MS*	*F*	*Sig. F*
Regression	4	6007.821	1501.955	59.7718	1.69E-10
Residual	19	477.435	25.12816		
Total	23	6485.256			

	Coeffs.	*Standard Error*	*t Stat*	*P-value*	*Lower 95%*	*Upper 95%*	*Lower 95.0%*	*Upper 95.0%*
Intercept	18.5336	1.64082	11.2953	7.15E-10	15.09932	21.96788	15.09932	21.96788
F_z	-14.2495	1.02323	-13.9259	2.02E-11	-16.3911	-12.1078	-16.3911	-12.1078
D_o	-3.2947	1.160238	-2.83968	0.01048	-5.72311	-0.86629	-5.72311	-0.86629
C_H	-2.96233	1.16024	-2.55321	0.019427	-5.39073	-0.53392	-5.39073	-0.53392
P_B	-4.71858	1.49786	-3.15021	0.00527	-7.85363	-1.58352	-7.85363	-1.58352

The ANOVA only shows that the experimental design as a whole is valid but all the factors considered in the design may not be relevant. The analysis following the ANOVA helps in determining the importance of all factors. The factors are analyzed on the basis of the corresponding *p-value* generated in the table. The *p-value* or calculated probability is the estimated probability of rejecting the null hypothesis of a study question when that hypothesis is true. If the *p-value* is less than the chosen significance level then the null hypothesis is rejected. In the current study, the null hypothesis is that none of the factors considered in the study are significant enough such that they may have an affect the peak jet velocity. The alternate

hypothesis is that one or more factors are significant and to identify these factors the corresponding *p-values* are considered. Conventionally for this analysis the 5% (less than 1 in 20 chance of being wrong) levels or the 95% confidence internal mark has be chosen such that the *p-value* has to be less than 0.05 (Devore 2004).

The *p*-values for F_z, D_o, C_H and P_B are found to be below the 0.05 goal at 2.02E-11, 0.0105, 0.0194 and 0.0053 respectively. For the fractional factorial design of Tab. 3 the other two factors, *E* and *f*, did not appear to be significant. This does not indicate that these factors can be eliminated completely. Interaction with main effects may be present but as the focus is only on linear models any additional effects are not taken into account in this study. Using Eq. (1), the average effect sizes for the selected factors are estimated as -28.499 for F_Z,-10.430 for D_o, -9.931 for C_H and -14.443 for P_B. For the remaining factors the effect sizes were 2.614 for *E* and 1.094 for *f*. Plots of all the effects showing the average responses are shown in Fig. 10.

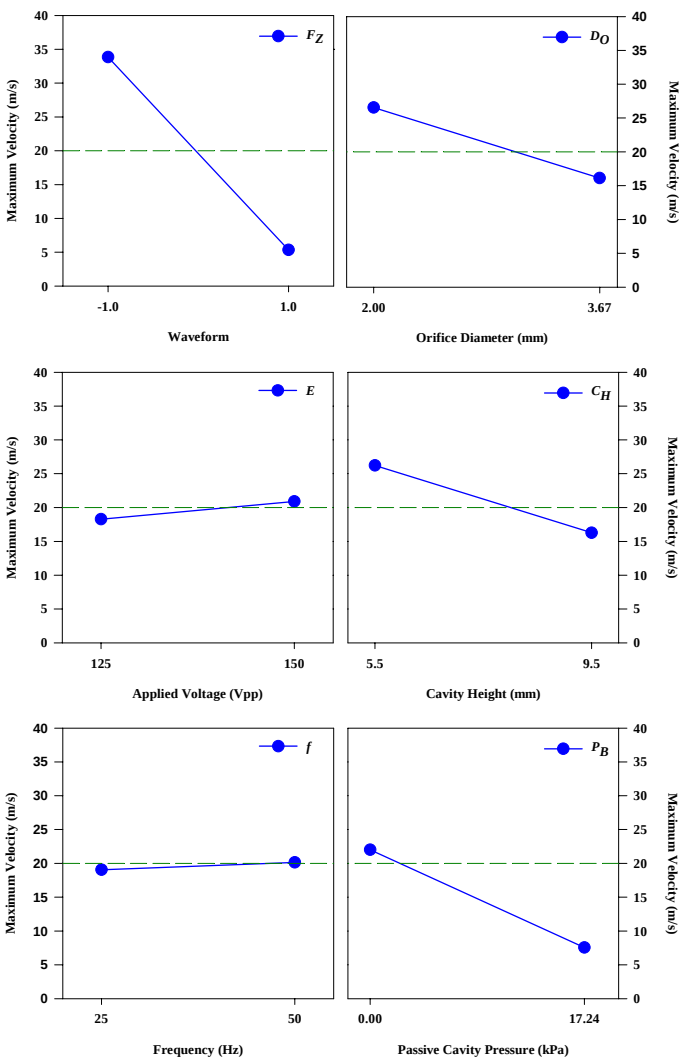

Figure 10Average factor effects

The main effects have large slopes as seen in the plots shown in Fig. 10 and the remaining factors have a small slope indicating that they do not have a significant role on the peak jet velocity.

Additional factors can be included using this approach to incorporate a number of factors such as, the cavity design, the covering plate thickness, the orifice shape, the size of the diaphragm, etc.

CONCLUSIONS

Bimorphs were studied as active diaphragms in synthetic jet cavities to investigate the effects of specific factors on the peak synthetic jet velocity, the response variable. Statistical analysis tools such as screening designs and fractional factorial models, were used to identify relevant factors chosen, namely driving signal used to excite the diaphragms, the magnitude and frequency of the signal, the volume of the cavity described by the cavity height, the size of the exit or orifice and the pressure in the passive cavity of the jet.

Results showed the driving signal has a significant effect on the peak jet velocities. The sawtooth driving signal produces much higher velocities in comparison with a sinusoidal waveform. Geometry of the cavity such as the cavity volume and the orifice size also has an effect on the peak velocity. The cavities with smaller volume produce higher velocity then larger volume cavities. Similarly the jets formed through smaller orifices have larger magnitudes then the larger orifice jets. With a sawtooth signal at larger frequencies a saturation effect is observed at the orifice such that the velocities increase up to 10Hz and reach a maximum thereafter. In case of a sine signal velocities continue to increase with increasing frequencies. The velocity is also affected by the magnitude of the driving signal, and it increases as the magnitude increases. In contrast the passive cavity pressure has an adverse effect on the jet with the velocities going down with an increase in passive pressure.

A regression analysis of the all results showed similar results. Amongst the six factors considered, the driving signal had the highest effect on the jet velocity and the factor of frequency proved to have very small effect. The cavity geometrical parameters also were relevant in each case. Finally, passive cavity pressure has a significant effect on jet velocity, diminishing the magnitude of the peak jet velocities obtained

ACKNOWLEDGMENTS

This project was sponsored through NASA grant NNL04AA04G.

REFERENCES

Amitay, M., Honohan, A., Trautman, M., and Glezer, A., 1997, “Modification of the Aerodynamic Characteristics of Bluff Bodies using Fluidic Actuators”, *AIAA*, 97–2004.

Amitay, M., Smith, B., and Glezer, A., 1998, "Aerodynamic flow control using synthetic jet technology," *AIAA*, 98–0208.

Bryant, R., G., 1996, ''LaRC-SI: A Soluble Aromatic Polyimide", *High Performance Polymers, Vol. 8*, No. 4, pp. 607–615.

Chen, Y., Liang, S., Aung, K., Glezer, A., Jagoda, J., 1999, "Enhanced Mixing in a Simulated Combustor Using Synthetic Jet Actuators," *AIAA*, 99–0449.

Collis, S., S., Joslin, R., D., Seifert, A., and Theofilis, V., 2004, "Issues in Active Flow Control: Theory, Control, Simulation, and Experiment," *Progress in Aerospace Science, Vol. 40*, pp. 237–289.

Crook, A., Sadri, A.,M. and Wood, N.,J., 1999, "The Development and Implementation of Synthetic Jets for the Control of Separated Flow," AIAA, 99–3176.

Davis, S. A., Glezer, A., 1999, "Mixing Control of Fuel Jets Using Synthetic Jet Technology : Velocity Field Measurement," AIAA, 99–0447.

Devore, J., L., 2004, "Probability and Statistics for Engineering and the Sciences," Duxbury Thomson Learning.

Dogan, A., Tressler, J., and Newnham, R., E., 2001, "Solid-State Ceramic Actuator Designs," *AIAA, Vol. 39*, No. 7.

Gad-el-Hak, M., 2000, "Flow Control: Passive, Active, and Reactive Flow Management," Cambridge University Press, Chapter 1.

Ho, C., H., and Tai, Y., C., 1996, "Review: MEMS and Its Applications for Flow Control", *Journal of Fluids Engineering, Vol. 118*, pp. 437–447.

John, J., E., A., 1984, "Gas Dynamics," Allyn and Bacon, 2nd Edition, pp 180.

Kral, L., D., Donovan, J.,F., Cain, A.,B., and Cary, A.,W., 1997, "Numerical Simulation of Synthetic Jet Actuators," 28th AIAA Fluid Dynamics Conference, 97–1824.

Liew, K., M., Lim, H., K., Tan, M., J., and He, X., Q., 2002, "Analysis of Laminated Composite Beams and Plates with Piezoelectric Patches using the Element-Free Galerkin Method," Computational Mechanics, Vol. 29, No. 6, pp. 486–497.

McLean, J., D., Crouch, J., D., Stoner, R., C., Sakurai, S., Seidel, G., E., Feifel, W., M., and Rush, H., M., 1999, "Study of the application of separation control by unsteady excitation to civil transport aircraft," NASA Technical Report, CR–1999–209338.

Montgomery, D., C., 2005, "Design and Analysis of Experiments," John Wiley & Sons Inc.

Mossi, K., Bryant, R., 2004a, "Pre-stressed Circular Actuators," American Ceramic Society, pp. 445–454.

Mossi, K., Bryant, R., G., 2004b, "Synthetic Jets for Piezoelectric Actuators," Materials Research Society, pp. 407–412.

Mossi, K., Mane, P., and Bryant, R., 2005a, "Velocity Profiles for Synthetic Jets Using Piezoelectric Circular Actuators", AIAA, 2005-2341.

Mossi, K., Castro, N., D., Bryant, R., and Mane, P., 2005b, "Boundary Condition Effects on Piezo-Synthetic Jets," Integrated Ferroelectrics, Vol. 71, pp. 257–266.

Rathnasingham, R., and Breuer, K., S., 1997, "System Identification and Active Control of a Turbulent Boundary Layer," Ph.D. Thesis, Massachusetts Institute of Technology, Boston, MA.

Seifert, A., Bachar, T., Koss, D., Shepshelovich, M., and Wygnanski, I., 1993, "Oscillatory Blowing: A Tool to delay Boundary-Layer Separation," AIAA Journal, Vol. 31, No. 11.

Seifert, A., Darabi, A., and Wygnanski, I., 1996, "Delay of Airfoil Stall by Periodic Excitation," Journal of Aircraft, Vol. 33, No. 4.

Smith, B., L., and Glezer, A., 1997, "Vectoring and Small Scale Motions Effected in Free Shear Flows Using Synthetic Jet Actuators," AIAA, 97–0213.

Smith, B., L., and Glezer, A., 1998, "The formation and evolution of synthetic jets," Physics of Fluids, Vol. 10, pp. 2281–2297.

Smith, B., L., 1999, "Synthetic Jets and their Interaction with Adjacent Jets," Ph.D. Thesis, Georgia Institute of Engineering, Atlanta, GA.